United States Department of the Interior

BUREAU OF RECLAMATION
PO Box 25007
Denver, Colorado 80225-0007

IN REPLY REFER TO:
86-68250
PRJ-13.00

Transmitted on 9/29/2016

VIA ELECTRONIC MAIL

MEMORANDUM

To: Lisa Krosley
Dam Safety Office

From: Kathleen D. Holman, Ph.D.
Flood Hydrology and Meteorology Group
Technical Service Center

KATHLEEN HOLMAN Digitally signed by KATHLEEN HOLMAN Date: 2016.09.30 08:52:43 -06'00'

Subject: Transmittal of "Characterizing Flood Seasonality in the Taylor Park Dam Watershed" Report

Please find attached the final report for the Dam Safety Office Technology Development Program project, Characterizing Flood Seasonality in the Taylor Park Dam Watershed. This report has been prepared by the Technical Service Center to fulfill the project requirements agreed upon in the submitted proposal documentation.

The report has been prepared by Kathleen D. Holman (Meteorologist) of Reclamation's Flood Hydrology and Meteorology Group. The report has been peer reviewed by Joseph M. Wright, in accordance with Technical Service Center Peer Review guidelines.

Please contact Kathleen Holman by phone at 303-445-2571 or via email at kholman@usbr.gov with any questions regarding this report.

Attachment

Hard Copy CC (w/att):
84-44000 (DSDams)

Electronic Copy CC (w/att):
84-44000 (Krosley)
86-68250 (Holman, Niehaus, Wright),
DSDaMS@usbr.gov
OfficialRecordsArchive@usbr.gov
KBartojay@usbr.gov
LKrosley@usbr.gov

RECLAMATION

Managing Water in the West

Characterizing Flood Seasonality in the Taylor Park Dam Watershed

Dam Safety Office Technology Development Program
Technical Memorandum 8250-2016-015 (DSO-2016-07)

U.S. Department of the Interior
Bureau of Reclamation

September 2016

Mission Statements

The U.S. Department of the Interior protects America's natural resources and heritage, honors our cultures and tribal communities, and supplies the energy to power our future.

The mission of the Bureau of Reclamation is to manage, develop, and protect water and related resources in an environmentally and economically sound manner in the interest of the American public.

Cover photo of Taylor Park Dam and reservoir, courtesy of Nicole Novembre.

Characterizing Flood Seasonality in the Taylor Park Dam Watershed

KATHLEEN HOLMAN Digitally signed by KATHLEEN HOLMAN Date: 2016.09.29 14:16:14 -06'00'

Prepared: Kathleen D. Holman, Ph.D. Date
Meteorologist
Flood Hydrology and Meteorology Group, 85-825000

JOSEPH WRIGHT Digitally signed by JOSEPH WRIGHT Date: 2016.09.29 14:20:05 -06'00'

Peer Review: Joseph Wright, P.E. Date
Hydrologic Engineer
Flood Hydrology and Meteorology Group, 85-825000

Executive Summary

Taylor Park Dam is the current subject of a hydrologic hazard analysis (HHA). The HHA is motivated by results from a 2005 Comprehensive Facility Review, which indicate that Taylor Park dam overtops at approximately 54% of the rain-on-snow probable maximum flood, based on a June general storm. Although the HHA will explore historical streamflow events for use in a flood-frequency analysis, an analysis of flood seasonality within the watershed, along with an explanation of potential meteorological causes is outside the scope and budget of the study. The purpose of the current project is to explore historical flood seasonality in the Taylor Park Dam watershed and identify antecedent conditions prior to major flooding events. We analyze historical observations of flow, precipitation, and snow water equivalent (SWE) in and surrounding the watershed.

Our results show that average daily flows into Taylor Park reservoir peak in June, May, and July. Average monthly precipitation, however, is lowest in June and greatest in August. SWE in the region typically peaks during March, April, and May, while the largest negative average daily changes in SWE occur during May. Annual maximum inflow events in the watershed occur most frequently during June and May, though there is large year-to-year variability in the flow magnitudes.

Composite analysis of land surface output from the Variable Infiltration Model, which is included in phase 2 of the National Land Data Assimilation System, suggests that the annual maximum inflow events in the Taylor Park Dam watershed can be described as rain-on-snow events. However, composite analysis captures "average" conditions. Consequently, additional research is needed to explore the annual maximum inflow events individually. There remains a possibility for other mechanisms (aside from rain-on-snow) to produce some of the annual maximum inflow events.

Table of Contents

List of Figures

List of Tables

1 Introduction

1.1 Background and Objectives

Taylor Park Dam, a zoned earthfill structure (Figure 1.1) located around 9,200 feet above sea-level west of Buena Vista, Colorado, is the current subject of a hydrologic hazard analysis (HHA). The HHA is motivated by results from a 2005 Comprehensive Facility Review, which indicate that Taylor Park dam overtops at approximately 54% of the rain-on-snow probable maximum flood, based on a June general storm (Collins et al. 2005). The flood related potential failure mode is overtopping erosion of the embankment during an extreme flood (USBR 2005). The Dam Safety Office requested the HHA in an effort to further understand the hydrologic risk at Taylor Park Dam.

Figure 1.1 - Photo of Taylor Park Dam looking upstream. Photo courtesy of Nicole Novembre.

Although the HHA will explore historical streamflow events for use in a flood-frequency analysis, a detailed analysis of flood seasonality within the watershed, along with an exploration of meteorological causes (including possible rain-on-snow events), is outside the scope and budget of the study. The purpose of the current project is to explore historical flood seasonality in the Taylor Park Dam watershed (Figure 1.2) and characterize antecedent conditions prior to major flooding events. The methods, datasets, and tools developed are applicable to any future hydrologic analysis, but may be most relevant to studies involving high-elevation, snowmelt-dominated watersheds.

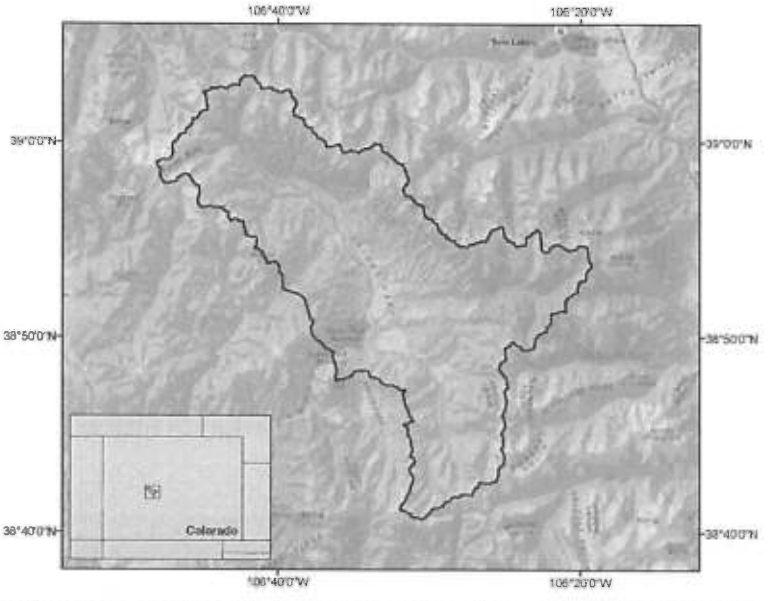

Figure 1.2 - Map of the Taylor Park Dam watershed (black outline), which drains 254 mi^2.

1.2 Previous Research

Flood frequency estimates are required for many water management and design engineering projects. Probabilistic estimates in some HHAs are developed by fitting a single statistical distribution to a sample of recorded flow maxima. However, the statistical functions only capture the aggregate effect of all flood-producing mechanisms, instead of providing an understanding of the underlying processes. Classifying floods based on the driving processes at an event level may support monitoring, assessment, and decision-making stages of the risk management process.

The physical interactions that give rise to floods of a given probability are controlled by a number of variables and processes, including seasonal variations in flood producing mechanism (e.g., convection, frontal systems, snowmelt), low-frequency climate variability (e.g., El Niño/Southern Oscillation) and catchment state and characteristics (Merz and Blöschl 2003). For example, along the Coquihall River in the Cascade Mountains, high spring flows are often associated with rising temperatures and little precipitation, while large winter flows are typically associated with heavy precipitation (Waylen and Woo 1982). Waylen and Woo (1982) use a single metric of four-day antecedent precipitation totals to distinguish between the two flood types; four-day antecedent precipitation totals less than 0.98 inches (25 mm) are associated with temperatures above 68 °F (20 °C), suggesting snowmelt driven events. The authors separate flood pools based on this antecedent precipitation metric and fit a separate Gumbel distribution to the two subsets. The authors then combine the results into a single Gumbel

distribution. Combining the two distributions enhances the fit of flood probabilities in regions where annual floods are produced by mixed processes.

Sui and Koehler (2001) explore flood events and the role of rain-on-snow using point observations from 17 gauging stations in a forested region of South Germany. Precipitation in this region reaches a maximum during summer, while flows reach a maximum during winter. The authors label heavy flow events as rain-on-snow induced if rain is observed while snow water equivalent decreases. Within the 170 top flow events (top 10 events from each station), more than 70% occurred from snowmelt combined with rainfall. The authors note that none of the 170 events resulted from snowmelt alone.

Unlike Waylen and Woo (1982) and Sui and Koehler (2001), who use surface observations of streamflow, precipitation, and SWE to categorize flooding events, Hirschboeck (1987) uses information on atmospheric circulation conditions to separate flooding events in the Gila River Basin, in Arizona. The author uses a detailed decision tree to assign flood events between 1950 and 1980 to one of nine hydroclimatic classifications. Those classifications include tropical storm (TS), cutoff low (C), front (F), monsoon front (MF), monsoon widespread precipitation (MW), monsoon local precipitation (ML), widespread precipitation (W), localized precipitation (L), snowmelt (S), and undefined flood (U). Figure 1.3 shows the monthly and total flood classifications for the Gila River Basin. Results indicate that frontal events occur most frequently between December and March, snowmelt floods typically happen during March and April, and monsoonal flood events primarily occur during the end of the summer (July and August). Together, frontal systems and monsoonal events account for approximately 73% of the flood events in this basin between 1950 and 1980.

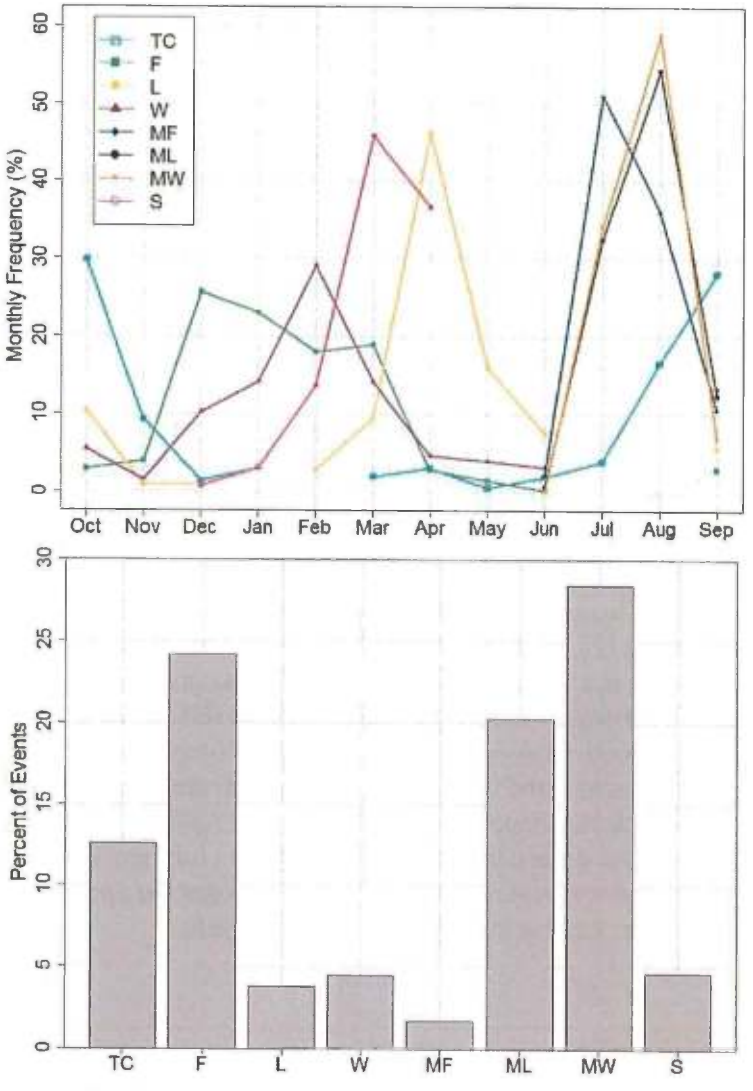

Figure 1.3 - (top) Monthly and (bottom) total frequency distribution (expressed as percentages) of hydroclimatic categories in the Gila River Basin between 1950 and 1980. Figure adapted from Hirschboeck (1987). See text for details.

Incorrectly assuming that all flood events have been sampled from a single population can have implications on flood frequency estimates (Elliott et al. 1982; Waylen and Woo 1982; Alila and Mtiraoui 2002). In the current study, we explore the seasonality of flooding events in the Taylor Park Dam watershed and characterize surface conditions surrounding these events in an effort to identify possible subgroups of flood mechanisms. Results from this study may be relevant to the existing hydrologic hazard analysis underway at Taylor Park and future flood frequency analyses in the Flood Hydrology and Meteorology Group.

2 Data and Methods

Historical data from a variety of sources are analyzed in an effort to characterize the seasonality of flooding events in the Taylor Park Dam watershed, along with the antecedent conditions prior to flooding events. The following sub-sections describe these data sources. This section also includes a description of the tools developed throughout this project.

2.1 Observations

In this study, we analyze historical observations of inflows to the Taylor Park reservoir, daily precipitation, and snow water equivalent (SWE). Daily historical inflow to the Taylor Park reservoir is computed by the Bureau of Reclamation's Upper Colorado River Office[1]. Computed inflows are analyzed instead of streamflow observations due to data continuity and period of record; the computed time series of daily inflow is continuous from October 1963 to present. The computed inflows represent naturalized flows, since the watershed is entirely undeveloped.

Daily precipitation observations are available through the GHCN-Daily dataset (Menne et al. 2012). The Park Cone station (GHCND:USS0006L02S – Park Cone, CO US; hereafter referred to as Park Cone) is the primary station of interest because the gauge is located inside the Taylor Park Dam watershed (Figure 2.1). Daily SWE observations are based on automated observations from the SNOw TELemetry (SNOTEL) network, which is maintained by Natural Resources Conservation Service (NRCS; NRCS 2009). This study requires SWE stations to have a minimum of 85% data coverage for nine or more years. In addition, for a SWE station to be included, the annual maximum SWE time series must be significantly correlated with the annual maximum time series of inflow to Taylor Park reservoir (not shown). Figure 2.1 shows the location of SWE gauges that meet these criteria. Elevation of the SWE gauges ranges from 8700 feet (2652 m) to 11440 feet (3487 m), with observations available from 1979 to 2015.

[1] http://www.usbr.gov/rsvrWater/faces/rvrOSMP.xhtml

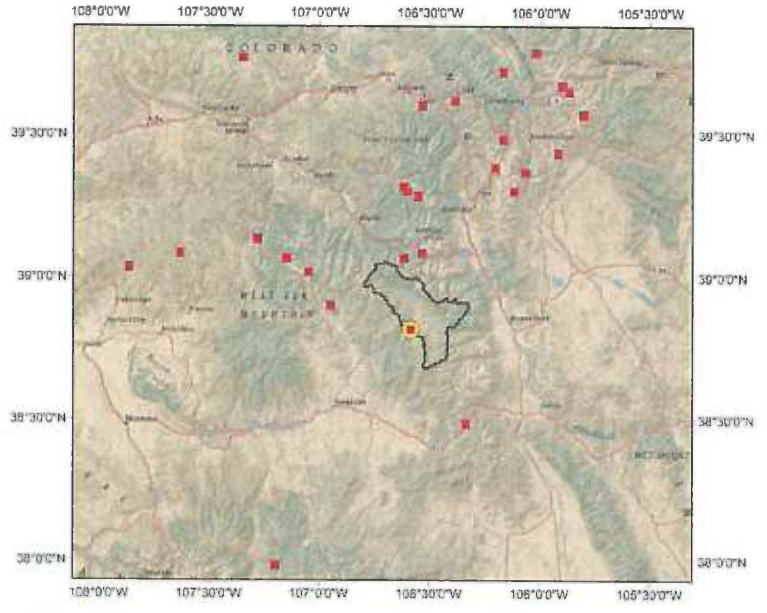

Figure 2.1 - Precipitation (yellow circle) and SWE (red square) gauges used in the analysis.

2.2 Gridded Data

In addition to point observations, we analyze gridded land surface model output from Phase 2 of the North American Land Data Assimilation System (NLDAS-2; Xia et al. 2012a, b). NLDAS-2 is an offline modeling system that runs four land models on a ⅛° grid over the continental U.S (Xia et al. 2015). Hourly gridded data are available from 1979 to present. The four land surface models include Noah, Mosaic, Sacramento soil moisture accounting (SAC-SMA), and the Variable Infiltration Capacity Model (VIC). The land surface models are forced by a combination of daily gauge-based precipitation observations and meteorological output from the North American Regional Reanalysis (NARR; Mesinger et al. 2006) dataset. The meteorological forcing data from NARR includes downward shortwave radiation, downward longwave radiation, 2 m air temperature, 2 m air specific humidity, surface precipitation, surface pressure, and 10 m wind speed.

The gauge-based precipitation and NARR fields are adjusted prior to use in the NLDAS framework. Daily gauge-based precipitation observations are temporally disaggregated to an hourly time step using satellite and radar observations (Xia et al. 2012a). The gauge-based precipitation fields are also bias corrected to match monthly precipitation totals from the Parameter-Elevation regressions on Independent Slopes Model (PRISM; Daly 1994). NARR data are spatially and temporally downscaled. The 2 m air temperature and 10 m specific humidity fields from NARR are adjusted for variations in topography. In addition, downward shortwave radiation from NARR is bias corrected using *GOES-8* retrievals (Pinker et al. 2003). Additional details on the preprocessing steps of

forcing data are available from the NCEP/Environmental Modeling Center NLDAS-2 website[2].

While NLDAS-2 data are available from four different land surface models, we present results based on the NLDAS-2 VIC model (Liang et al. 1999). The NLDAS-2 VIC configuration was selected for analysis and presentation because other members of the Flood Hydrology and Meteorology Group are familiar with the VIC model. Future research may explore output from the remaining three land surface models available through the NLDAS-2 framework.

2.3 Tools

The current project developed a number of valuable tools (in the form of computer scripts) to download, process, analyze, and plot the various datasets discussed previously. This section provides a brief review of those scripts (Table 2.1) and the primary methods used in this study. Three different software languages were used to produce scripts, including R (R Core Team 2016), the NCAR Command Language (NCL; NCL 2016), and bash[3], a UNIX shell. Not all scripts produced are listed in Table 2.1. However, copies of any or all scripts are available from the author upon request.

[2] http://www.emc.ncep.noaa.gov/mmb/nldas/LDAS8th/forcing/forcing_narr.shtml
[3] https://en.wikipedia.org/wiki/Bash_(Unix_shell)

Table 2.1 - Brief description of scripts developed in this project.

Language	Description
R	Analyze and plot daily inflow, precipitation, and SWE observations
NCL	Calculate monthly correlations, spatial correlations, and lead/lag correlations between daily inflow data and the Livneh et al. (2013) dataset (not shown)
R	Automate the process to create wget scripts
Bash	Download land surface model output from NLDAS-2
NCL	Convert NLDAS-2 files from WMO GRIB-1 format to NetCDF
Bash	Concatenate hourly NLDAS-2 files into daily files
Bash	Verify the number of hours in each daily NLDAS-2 file
NCL	Extract smaller domain from the CONUS-wide NDLAS-2 files and save data to NetCDF format
NCL	Compute daily averages from hourly files
NCL	Calculate monthly correlations, spatial correlations, and lead/lag composites between daily inflow data and NLDAS-2 output
R	Plot basin-wide average composite values of precipitation, skin temperature, and SWE
R	Analyze and plot historical soil moisture observations from the National Resources Conservation Service (not shown)
R	Perform regionalized L-moments analysis on historical SWE observations (not shown)

Results presented in this report take the form of box and whisker plots and spatial maps from composite analysis. The box and whisker plots, also called boxplots, are used to display a distribution of data points. Unless otherwise stated, the thick horizontal black lines (inside grey boxes) represent the median and the red vertical dashed lines represent the 10^{th} and 90^{th} percentile values from the distribution of data points (see Figure 2.2). The upper and lower bounding lines of the grey boxes represent the 75^{th} and 25^{th} percentiles, respectively. Black squares, where present, represent the long-term average.

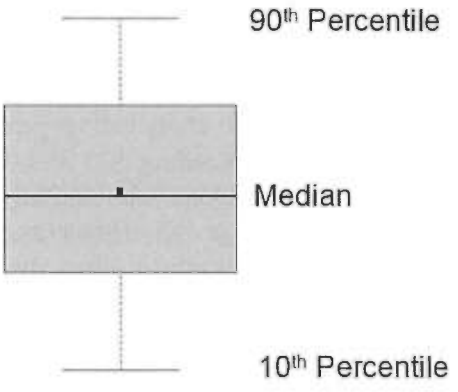

Figure 2.2 - Example boxplot with parameters labeled.

Composites analysis, a method used to describe "average" conditions surrounding a set of events, is also used in this project. The set of events used to develop a composite is referred to as the basis. In this study, the basis is annual maximum daily inflow events to the Taylor Park reservoir. We explore average surface conditions surrounding annual maximum inflow events based on historical output from NLDAS-2 VIC simulations. These composites are referred to as lead/lag composites. Negative lag values (e.g., day -6) indicate composites based on conditions prior to basis events, while positive lead values (e.g., day +6) indicate composites based on conditions after basis events. In this study, negative lag values represent surface conditions that occurred prior to annual maximum inflow events (i.e., flow leads). Positive lag values represent surface conditions that occurred after the annual maximum inflow event (i.e., flow lags).

3 Results

Average daily inflow to the Taylor Park reservoir is characterized by a strong seasonal cycle (Figure 3.1). On average, daily inflow peaks during June, May, and July, with average daily inflows exceeding 300 ft^3/s during these months. Daily flows during the remainder of the year are relatively low, with magnitudes less than 165 ft^3/s. Variability in average daily flows (as measured by the standard deviation of daily inflows by month) follows the same seasonal cycle.

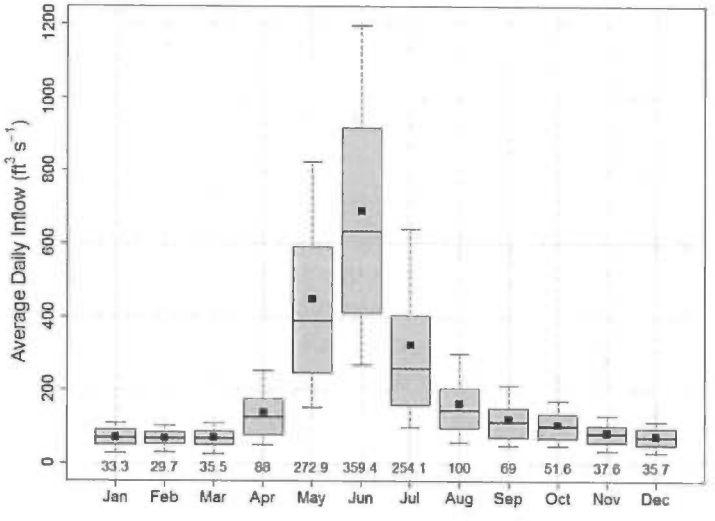

Figure 3.1 - Box and whisker plot of average daily inflow (ft^3/s) to the Taylor Park Dam reservoir between 1962 and 2015. The blue number above each month represents the standard deviation of average daily inflow.

The seasonal cycle of extreme inflow events into Taylor Park reservoir strongly resembles the seasonal cycle of average daily inflows. Figure 3.2 shows the frequency distribution of top inflow events (top 50%, 25%, 10%, 5%, and 1% of all days in the record) to the reservoir by month. For example, majority of the top 25% of inflow events occur between May and August, with the largest fraction occurring during June. As the intensity of events increases (e.g., the top 10%, top 5%), the timing remains constrained to the months of May, June, and July. Alternatively, the timing of the top 50% of events (i.e., the top half of the data record) is relatively disperse, with May having the largest percentage. This disperse behavior is likely the result of the high autocorrelation in daily inflows.

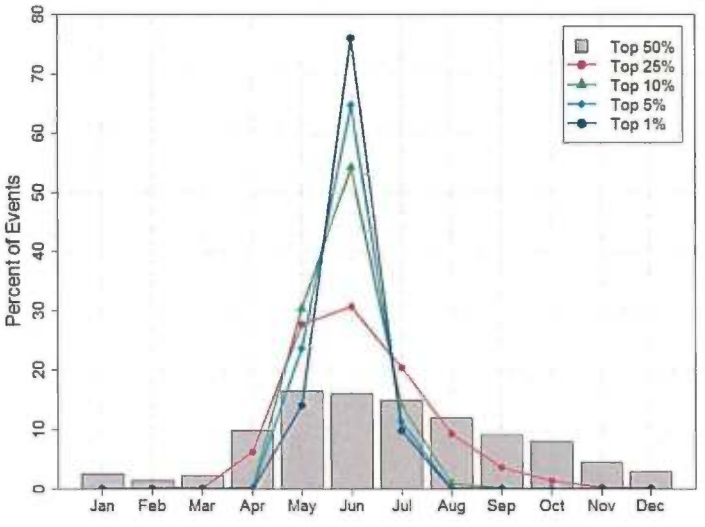

Figure 3.2 - Average monthly frequency distribution (expressed as %) of top daily inflow events to the Taylor Park Dam reservoir between X and Y.

Unlike average daily inflows, average monthly precipitation at the Park Cone gauge (Figure 3.3) is not characterized by a strong seasonal cycle. Instead, average monthly precipitation totals range from 1.38 in June to 2.20 in February and August. Variability in monthly totals peaks during August and December, with minimums during the transition seasons (spring and fall).

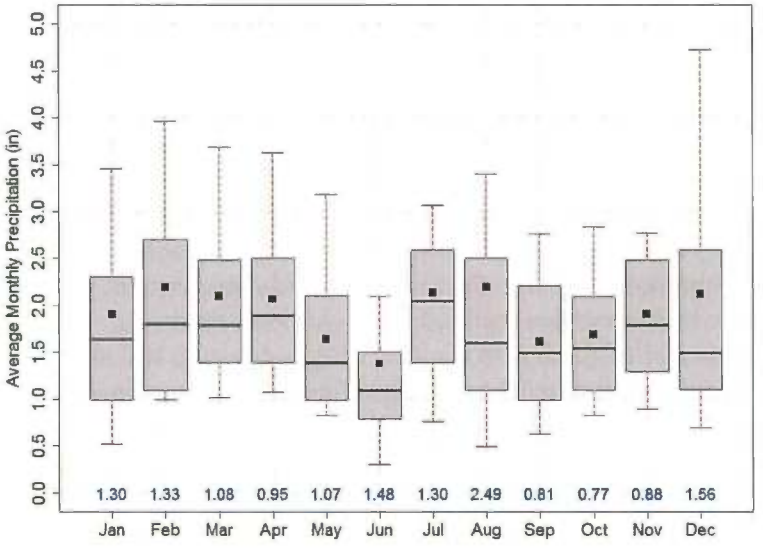

Figure 3.3 - Box and whisker plot of average monthly total precipitation (in) at the Park Cone gauge between water years 1981 and 2014. The blue number above each month represents the standard deviation of monthly total precipitation.

The seasonality of extreme precipitation events at Park Cone share some similarities with the seasonal cycle of average monthly precipitation (Figure 3.4).

For example, the top 10% and top 5% of daily precipitation totals (including non-precipitating days, N=1242 and 621, respectively) tend to occur during late summer (July and August) and spring (March and April). The spring events likely fall as solid precipitation, because of the high elevation location of Taylor Park. The frequency distribution of the top 1% of daily precipitation totals (N=124) shows a different seasonality, with three primary peaks throughout the year. Top 1% of events primarily occur during February, July, and December. These three months account for approximately 36% of the top 1% of events.

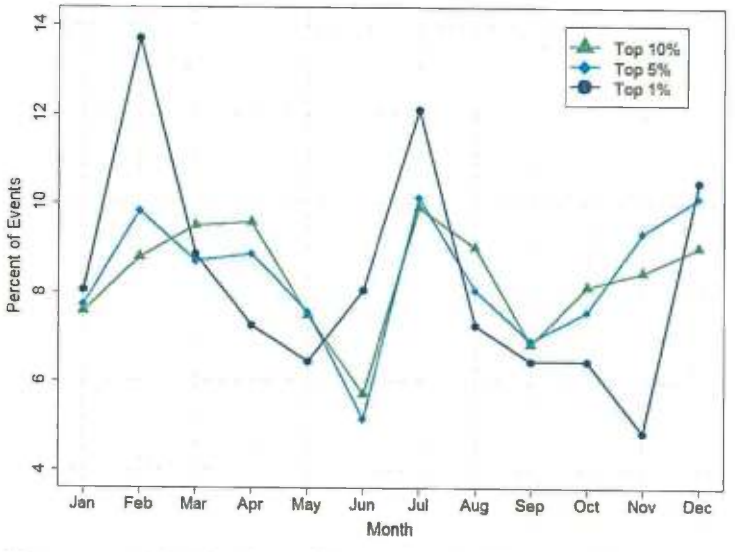

Figure 3.4 - Frequency distribution of the top 10%, 5%, and 1% of daily precipitation totals at the Park Cone gauge between water years 1981 and 2014.

Clearly, the dominant seasonal cycle of average daily inflow to the Taylor Park reservoir is inconsistent with the seasonal cycle of average monthly precipitation totals. The same is true regarding extreme daily inflow events and heavy precipitation events, suggesting an alternative moisture source for the large late-spring/early-summer flows into the reservoir. This inconsistency is not surprising because of the high elevation location of Taylor Park reservoir. Previous studies show that large and extreme flows in many high-elevation watersheds are controlled by processes other than precipitation, such as snowmelt and rain-on-snow (Jarrett and Costa 1988; Merz and Blöschl 2003; McCabe et al. 2007). We explore the relationship between SWE and daily flows using observations located within and surrounding the Taylor Park Dam watershed.

On average, the snow accumulation season in the region of Taylor Park Dam watershed starts in September (Figure 3.5). Average daily SWE totals typically increase from September through March and April, when average daily totals peak. Average daily totals typically decline from April through July. Figure 3.6 shows monthly distributions of changes in daily SWE from the same sites included in Figure 3.5, where the changes were computed as a forward difference

(i.e., SWE_{d+1}-SWE_d). Results in Figure 3.6 agree with the findings in Figure 3.5; daily SWE totals begin to decline in April, with May demonstrating the largest average changes in daily SWE totals. The largest average changes in daily SWE occur one month prior (May) to the month of largest average daily inflows to the Taylor Park reservoir (June), suggesting that snowmelt may play a vital role in annual maximum flows.

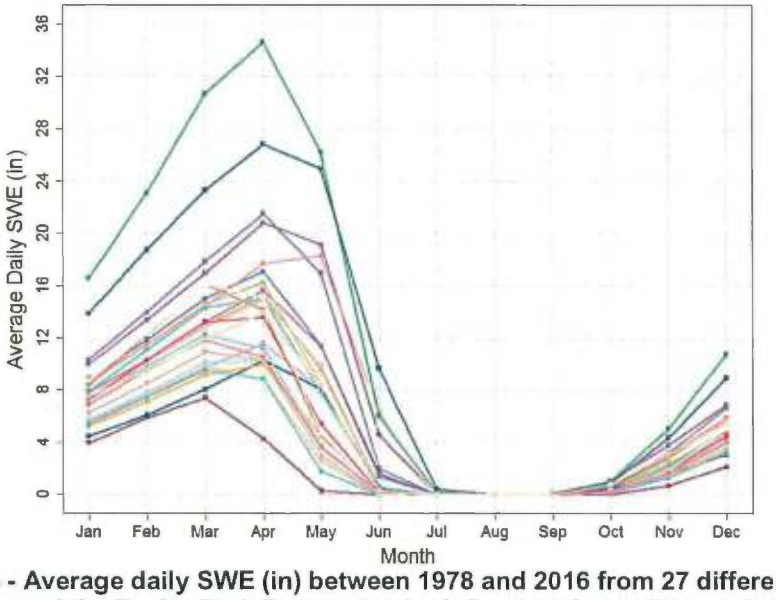

Figure 3.5 - Average daily SWE (in) between 1978 and 2016 from 27 different sites located around the Taylor Park Dam watershed. See text for additional details.

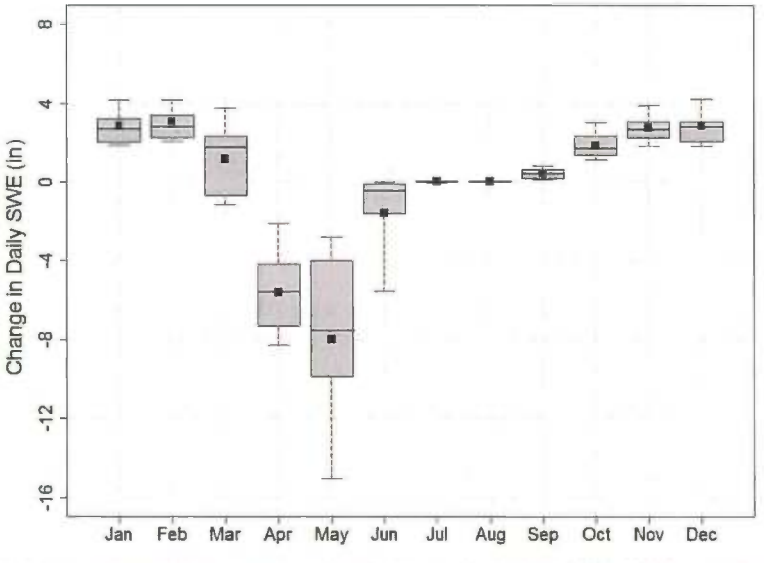

Figure 3.6 - Box and whisker plot of the change in daily SWE (in) based on the gauges shown in Figure 2.1.

In addition to exploring the seasonality of average daily inflows to Taylor Park reservoir, we explore the seasonality and mechanisms of annual maximum inflow events. Annual maximum inflow events are vital in flood frequency analyses used in most HHAs. Figure 3.7 shows the time series of annual maximum daily inflow events to the Taylor Park reservoir between water years 1963 and 2015. The full table of events is available in Appendix A. Each data point is colored by the month of occurrence. Annual maximum daily inflows range from 292 ft^3/s on 20 May 2002 to 2427 ft^3/s on 18 June 1995, with a long-term average of 1144 ft^3/s. Approximately 55% of the annual maximum daily inflow events occur during June. During the 53 years of observations, the annual maximum daily inflow event occurred during the month of July one time. Figure 3.7 shows that there is a great amount of year-to-year variability in annual maximum inflow events to the Taylor Park reservoir.

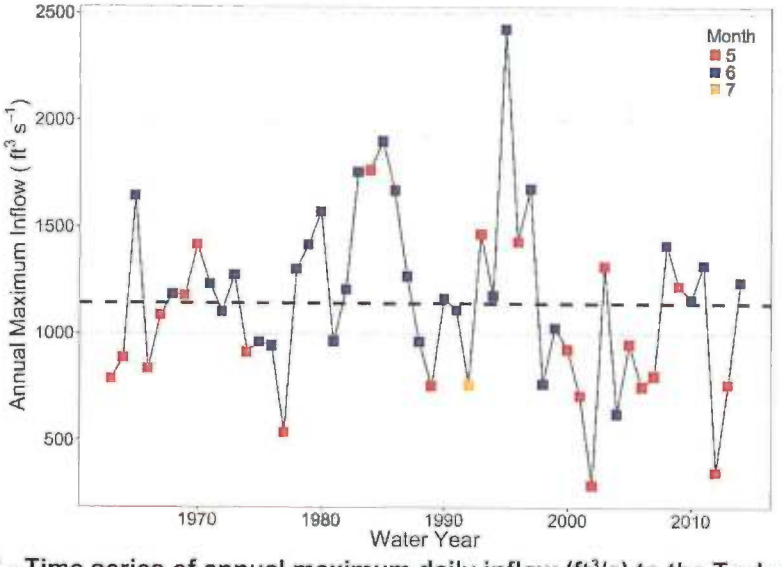

Figure 3.7 - Time series of annual maximum daily inflow (ft^3/s) to the Taylor Park reservoir between water years 1963 and 2014. Node color represents the month of maximum occurrence. The dashed horizontal line represents the long-term average (1144 ft^3/s).

Lead/lag composites represent a convenient way of characterizing surface conditions prior to, during, and after a series of events. Figure 3.8, Figure 3.9, and Figure 3.10 show lead/lag composites of daily total precipitation (mm; frozen plus unfrozen), skin temperature (°F), and SWE (mm), respectively, starting six days prior to and ending three days after the annual maximum inflow events to the Taylor Park reservoir between 1979 and 2014 based on output from NLDAS-2 VIC simulations. Negative (positive) lags represent surface conditions prior (after) to annual maximum events.

Composites of daily precipitation in Figure 3.8 suggest that precipitation is not a major source of water to the annual maximum inflow events. Average daily

precipitation totals in the watershed are less than 2.5 mm during each day leading up to and on the annual maximum inflow events. There is some precipitation to the west of the basin on day 0, with average values less than 3.5-4 mm. The top panel of Figure 3.11 shows a time series of basin-average (the domain is indicated by the black box in Figure 3.8) daily precipitation starting six days prior to the annual maximum events and ending six days after the annual maximum events (for a total of 13 days). This time series indicates that basin-average daily precipitation is greater than zero during every day shown and peaks on day -1 at 2.5 mm.

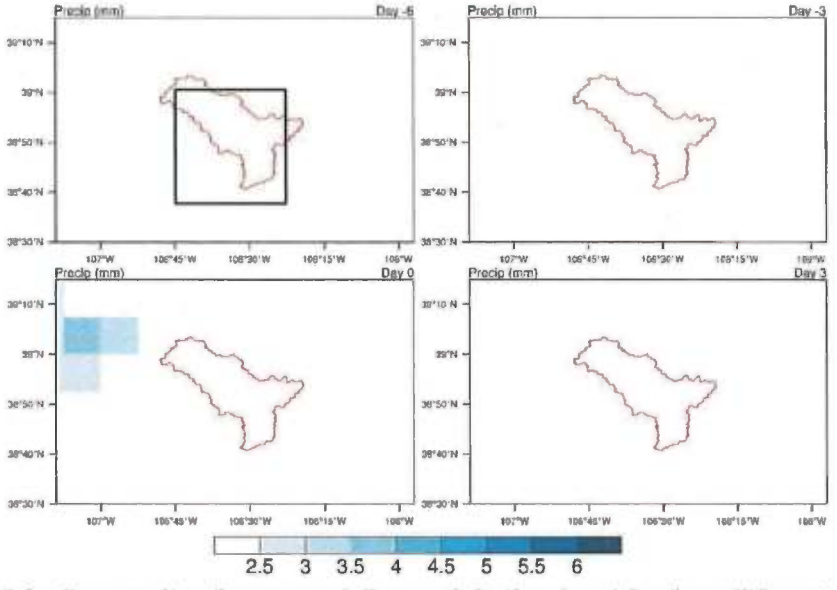

Figure 3.8 - Composite of average daily precipitation (mm) for four different lead/lag values.

Figure 3.9 shows lead/lag composites of skin temperature, the average temperature of all vegetation, bare soil, and snow skin temperatures within a grid cell. According to these results, skin temperatures in and surrounding the watershed increase from day -6 to day 0 and decrease from day 0 to day +3. Basin-average skin temperatures (middle panel of Figure 3.11) increase rapidly from day -6 to day -1, remain relatively constant from day -1 to day +3, and increase again from day +3 to day +6. The change in temperature between day -6 and day -1 is 3.7 °F. Average daily skin temperatures are above freezing during each of the 13 days, suggesting (but not proving) that the precipitation is likely falling as liquid.

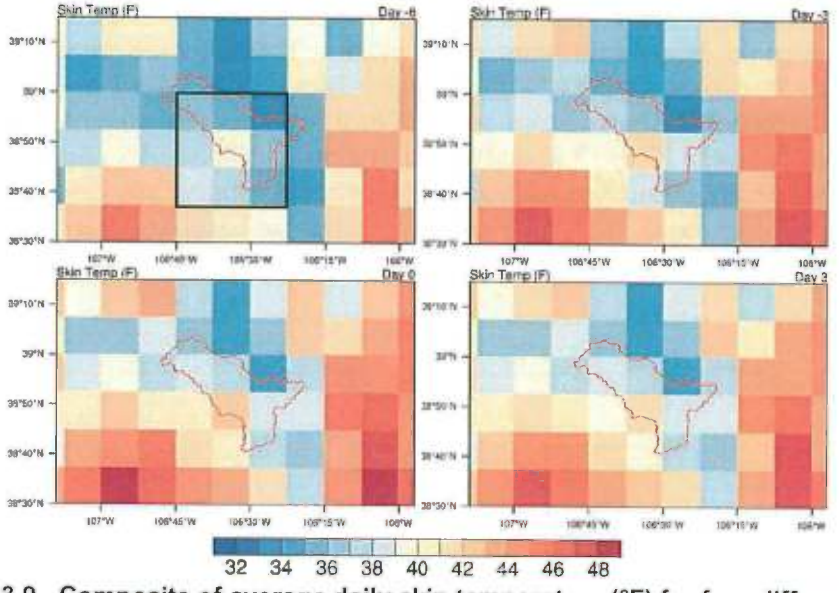

Figure 3.9 - Composite of average daily skin temperature (°F) for four different lead/lag values surrounding annual maximum inflow events to Taylor Park reservoir between 1979 and 2014.

Average daily composites of SWE in Figure 3.10 highlight the significance of snowmelt to annual maximum inflow events to the Taylor Park reservoir. Major declines in SWE within and surrounding the watershed are apparent from day -6 to day 0 and beyond. Six days prior to the annual maximum inflow events, basin-average SWE is 110 mm (bottom panel of Figure 3.11). Three days later, basin-average SWE declines to approximately 92 mm. By day 0 (the day of annual maximum inflow events), basin-average SWE declines to approximately 70 mm, a 36% reduction from day -6. Basin-average SWE continues to decline up to six days after the annual maximum inflow events.

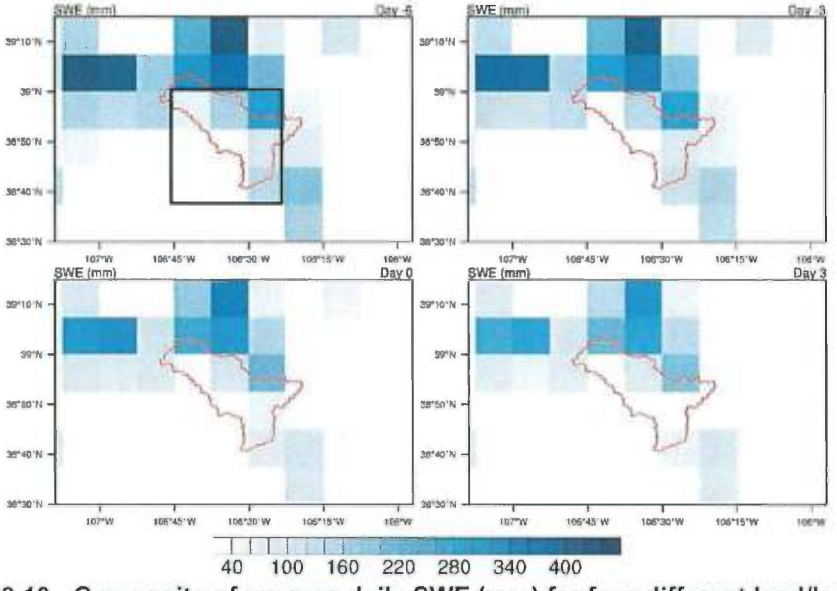

Figure 3.10 - Composite of average daily SWE (mm) for four different lead/lag values.

Basin-average lead/lag composites of precipitation, skin temperature, and SWE in Figure 3.11 broadly demonstrate the importance of precipitation and snowmelt to annual maximum inflow events to Taylor Park reservoir. As mentioned previously, Sui and Koehler (2001) categorize flood events as rain-on-snow driven if precipitation, specifically rain, is observed while SWE declines. We have demonstrated using composite analysis that basin-average total precipitation is non-zero every day leading up to and after the annual maximum inflow events. This precipitation likely falls as liquid since basin-average skin temperatures increase during the same period. Additional research on liquid and solid precipitation, as well as air temperatures, is needed to fully verify that events are indeed rain-on-snow events.

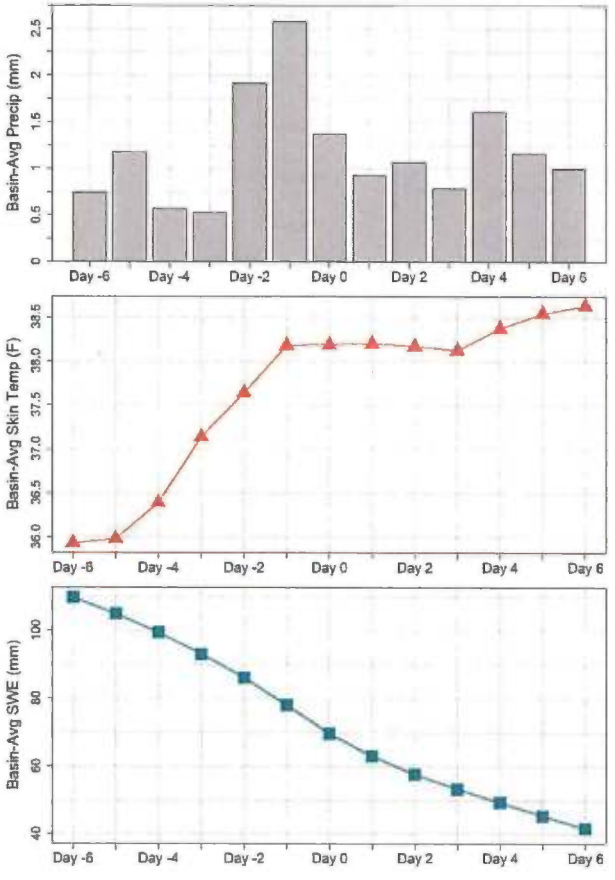

Figure 3.11 - Basin-average composites of (top) daily precipitation (mm), (middle) skin temperature (°F), and (bottom) SWE (mm) for 13 different lead/lag values surrounding annual maximum inflow events to Taylor Park reservoir. Positive (negative) day values on the x-axis represent conditions after (before) the annual maximum inflow event.

4 Summary and Conclusions

Taylor Park Dam is currently the subject of a Dam Safety hydrologic hazard analysis, motivated by results from a 2005 study that suggest the dam overtops at 54% of the rain-on-snow probable maximum flood. The purpose of the HHA is to produce updated flood routings that will be routed through the reservoir to improve estimates of overtopping potential. While the HHA explores historical streamflow events for use in a flood-frequency analysis, a detailed analysis of flood seasonality within the watershed, along with an explanation of meteorological causes (including possible rain-on-snow events), is outside the scope and budget. The objectives of this study are to explore historical flood seasonality in the Taylor Park Dam watershed and characterize antecedent conditions prior to the major flooding events, including surface conditions (e.g. snowpack). These objectives are accomplished using a combination of historical observations in and surrounding the watershed (inflow, precipitation, and SWE) and hourly gridded output from a land surface model (NLDAS-2 VIC).

Average daily flows into Taylor Park reservoir typically peak during June, with May second, and July third. Average flows during the remainder of the year are relatively low, with average magnitudes less than 165 ft^3/s. The heaviest flows, such as the top 1% of events and annual maximums, occur most frequently during the late spring/early summer (June, May, and July). Average monthly precipitation totals, however, are not characterized by a late spring/early summer peak. Instead, average monthly precipitation totals are lowest during June and greatest during August. Heavy precipitation events, such as the top 1% of daily totals, occur during February, July, and December. February and December events likely take the form of solid precipitation, due to the high elevation location.

Differences in the seasonality of average daily flows and monthly precipitation totals (as well as extreme flows and precipitation) suggest that precipitation may not be the sole source of moisture for heavy inflow events to the reservoir. Because of the high elevation, SWE is more likely to play a key role. Average daily SWE totals from 27 observations sites in the region typically increase from September to March. Daily changes in average SWE are predominantly negative between April and June, with the largest declines observed during May. The largest declines in daily SWE typically occur one month prior to the month (June) with the largest daily inflows to the reservoir.

Composite analysis of surface conditions from NLDAS-2 VIC simulations is used to demonstrate the importance of SWE and snowmelt to annual maximum inflow events. Results show that basin-average skin temperatures increase from day-6 to day -1, at which point they remain relatively steady until they begin to increase around day +3. Basin-average precipitation, which likely falls as liquid, is non-zero throughout this period, with a peak on day -1. Basin-average SWE however, declines every day prior to the annual maximum inflow events (and beyond).

While the composite analysis suggest that these events are likely rain-on-snow events, the mechanism(s) for any given year differs from these average composites. Additional research is needed to better understand mechanisms for each event individually, as sub-groups are more important for flood-frequency analyses than the collection of annual events that arise due to different hydrometeorological conditions and mechanisms (Alila and Mitiraoui 2002).

5 Acknowledgements

This report was prepared by Kathleen D. Holman, Ph.D., Meteorologist in the Flood Hydrology and Meteorology Group of the Bureau of Reclamation's Technical Service Center in Denver, Colorado. Joseph Wright, P.E., also in the Flood Hydrology and Meteorology Group, performed peer review.

6 References

Alila, Y. and A. Mtiraoui, 2002: Implications of Heterogeneous Flood-Frequency Distributions on Traditional Stream-Discharge Prediction Techniques. *Hydrological Processes*, **16** (5), 1065-1084.

Bales, R. C., N. P. Molotch, T. H. Painter, M. D. Dettinger, R. Rice, and J. Dozier, 2006: Mountain Hydrology of the Western United States. *Water Resour. Res.*, **42**, 1-13.

Collins, C. D., J. E. Klawon, and K. Bullard, 2005: Taylor Park Dam Comprehensive Facility Review Hydrologic Hazard. Department of the Interior, Bureau of Reclamation, Technical Services Center, Denver, CO.

Daly, C., 1994. *PRISM, Parameter-Elevation Regression on Independent Slopes Model.* Oregon State University, Oregon Climate Service, Corvallis, Oregon.

Elliott, J. G., R. D. Jarrett, and J. L. Ebling, 1982: Annual Snowmelt and Rainfall Peak-Flow Data on Selected Foothills Region Streams, South Platte River, Arkansas River, and Colorado River Basins, Colorado, Tech. Rep., United States Geological Survey.

Jarrett, R. D., and J. E. Costa, Evaluation of the Flood Hydrology in the Colorado Front Range using Precipitation, Streamflow, and Paleoflood Data for the Big Thompson River Basin, Tech. rep., United States Geological Survey, Reston, VA, Water Resources Investigations Report 87-4117, 1988.

Liang, X., D. P. Lettenmaier, E. F. Wood, and S. J. Burges, 1994: A Simple Hydrologically Based Model of Land Surface Water and Energy Fluxes for GCMs. *J. Geophys. Res.*, **99**, 14415–14428, doi:10.1029/94JD00483.

McCabe, G. J., M. P. Clark, and L. E. Hay, 2007: Rain-On-Snow Events in the Western United States. *Bull. Amer. Meteor. Soc.*, **88**, 319-328. doi: 10.1175/BAMS-88-3-319.

Menne, M. J., I. Durre, R. S. Vose, B. E. Gleason, and T. G. Houston, 2012: An Overview of the Global Historical Climatology Network-Daily Database. *J. Atmos. Oceanic Technol.*, **29**, 897-910, doi: 10.1175/JTECH-D-11-00103.1.

Merz, R., and G. Blöschl, Regional Flood Risk - What are the Driving Processes? International Association of Hydrological Sciences, Publication 281, 49–58, 2003

Mesinger, F., and Coauthors, 2006: North American Regional Reanalysis. *Bull. Amer. Meteor. Soc.*, **87**, 343-360.

The NCAR Command Language (NCL; Version 6.3.0) [Software], 2016: Boulder, Colorado: UCAR/NCAR/CISL/TDD. http://dx.doi.org/10.5065/D6WD3XH5

Pinker, R. T., and Coauthors, 2003: Surface Radiation Budgets in Support of the GEWEX Continental-Scale International Project (GCIP) and the GEWEX Americas Prediction Project (GAPP), Including the North American Land Data Assimilation System (NLDAS) Project. *J. Geophys. Res.*, **108**, 8844, doi:10.1029/2002JD003301.

R Core Team, 2016: R: A language and environment for statistical computing. R Foundation for Statistical Computing, Vienna, Austria. URL https://www.R-project.org/

Sui, J. and G. Koehler, 2001: Rain-on-Snow Induced Flood Events in Southern Germany. *J. Hydrology*, **252**, 205-220.

United States Bureau of Reclamation (USBR), 2005: Decision Memorandum, Comprehensive Facility Review - Taylor Park Dam - Uncompahgre Project. Technical Service Center, Denver, CO.

Waylen, P. and M.-k. Woo, 1982: Prediction of Annual Floods Generated by Mixed Processes. *Water Resour. Res.*, **18** (4), 1283–1286, 1982.

Xia, Y., and Coauthors, 2012a: Continental-Scale Water and Energy Flux Analysis and Validation for the North American Land Data Assimilation System Project Phase 2 (NLDAS-2): 1. Intercomparison and Application of Model Products, Journal of Geophysical Research: Atmospheres, 117 (D3).

Xia, Y., and Coauthors, 2012b: Continental-Scale Water and Energy Flux Analysis and Validation for the North American Land Data Assimilation System Project Phase 2 (NLDAS-2): 2. Validation of Model-Simulated Streamflow, Journal of Geophysical Research: Atmospheres, 117 (D3).

Xia, Y. M. B. Ek, Y. Wu, T. Ford, and S. M. Quiring, 2015: Comparison of NLDAS-2 Simulated and NASMD Observed Daily Soil Moisture. Park I: Comparison and Analysis. *J. Hydrometeo.*, **16**, 1962-1980.

Appendix A. Annual Maximum Inflow Events

Year	Month	Day	Inflow (ft^3/s)
1963	5	22	790.64
1964	5	22	886.41
1965	6	24	1646.87
1966	5	23	837.31
1967	5	24	1087.33
1968	6	4	1186.53
1969	5	31	1180.56
1970	5	27	1418.93
1971	6	22	1234.62
1972	6	6	1104.51
1973	6	15	1277.43
1974	5	30	913.68
1975	6	16	962.99
1976	6	10	944.74
1977	5	7	537.75
1978	6	16	1304.82
1979	6	15	1417.85
1980	6	13	1572.29
1981	6	8	964.11
1982	6	19	1210.18
1983	6	20	1758.15
1984	5	25	1768.39
1985	6	8	1902.94
1986	6	7	1671.44
1987	6	10	1271.12
1988	6	5	961.02
1989	5	31	756.12
1990	6	6	1167.56
1991	6	15	1110.58
1992	7	4	760.36
1993	5	27	1469.54
1994	6	3	1180.07
1995	6	18	2426.81
1996	5	18	1432.34
1997	6	8	1682.02
1998	6	3	766.2

1999	6	15	1030.54
2000	5	30	926.12
2001	5	28	709.66
2002	5	20	291.96
2003	5	30	1320.05
2004	6	8	626.95
2005	5	24	949.87
2006	5	23	752.58
2007	5	20	803.05
2008	6	3	1416.89
2009	5	19	1224.43
2010	6	7	1162.14
2011	6	17	1323.01
2012	5	23	352.38
2013	5	27	764.93
2014	6	4	1246.01